

Electrohydraulic full-forward extrusion of small parts through high aspect ratio forming channels

**L. Langstädtler^{1,2,3*}, M. Herrmann^{1,2,3}, C. Schenck^{1,2,3},
B. Kuhfuss^{1,2,3}**

¹ Bremen Institute for Mechanical Engineering (bime), Badgasteiner Straße 1, 28359 Bremen, Germany

² MAPEX - Center for Materials and Processing

³ University of Bremen, Germany

* Corresponding author. Email: langstaedtler@bime.de

Abstract

Electrohydraulic incremental bulk forming was introduced as a novel micro part forming technology. Forming of parts from different materials and different initial diameter values was investigated in single-stage full-forward extrusion in recent work. In this paper, multi-stage extrusion in high aspect ratio forming channels is presented. Thereby, the aspect ratio of forming channel is high, when the channel length is much higher than the channel diameter and formed part length. Analytical and experimental investigations are carried out to correlate the supplied and required energy for extrusion. Experiments were made using an optical access made of sapphire as part of the extrusion channel to measure the position during forming increments. The influence of channel depth and curvature as well as of fluctuations in the transmitting media on the energy transmission to the formed EN AW-6061 aluminum alloy parts were found to be low.

Keywords

Micro production, impulse bulk forming, optical process monitoring

1 Introduction

Sheet and bulk forming processes for micro parts are conventionally performed with solid stamps. Clearances in micro forming between stamp and die are small and even negative for fine blanking (Fan et al., 2012), which results in time and cost intensive tooling and risk of abrasion (Vollertsen et al., 2020). By small stamp diameter and relatively high forming forces, the stamps tend to break due to material limits. As solid stamps are unable to adapt to diameter changes, multi-stage forming is realized in transfer systems using several sets of stamps and

dies. This additionally increases expenses in tooling and handling, which is a general challenge in micro forming due to adhesion by high surface to mass ratio (Mahshid et al., 2014).

Some processes like rubber pad forming (Liu et al., 2010) or electromagnetic forming (Langstädtler et al., 2016) replace one side of the tool by a flexible stamp for micro forming applications. However, these processes were applied to forming thin sheet metals. A process which enables a flexible stamp for massive forming is hydrostatic extrusion. Thereby, a fluid is located between rigid stamp and micro part in the die. This fluid transfers the force and reduces friction between punch, part and die (Lange, 1993). However, for this process high static pressures up to gigapascals are required. Hence, beneath high rigidity of the die, adequate sealing between fluid and die as well as between part and die is required. Furthermore, the parts are formed slowly.

Electrohydraulic incremental micro forming was introduced as a material testing method. Testing of spherical as well as cylindrical micro samples with initial diameters between 0.6 mm and 2.0 mm was successfully performed. As the forming energy was not transferred within one step, extrusion was achieved incrementally (Langstädtler et al., 2018). Shock waves adapted to the changing shapes of samples and die and pushed the micro samples through the die. These forming operations were successfully performed with different sample materials and different load cases (Langstädtler et al., 2021).

Electrohydraulic full-forward extrusion through high aspect ratio forming channels enables micro production with simplified tooling and handling. In this context 'aspect ratio' means the ratio of channel diameter to channel length, as well as the ratio of sample length to channel length. One of the main challenges, i.e. sealing of split dies, was overcome by simplified manufacturing of channel elements. In contrast to extrusion with quasi-static loads, the processing was successfully without radial preload of the die and even without sealing of the joints. Furthermore, the segmented dies enabled unloading of the samples (Langstädtler et al., 2019) and the integration of an optical access (sapphire pane) for monitoring purpose (Stöbener et al., 2020). Different forming channels were designed for single and multi-stage extrusion.

In electrohydraulic extrusion, shock wave energy is transferred to forming energy. Assuming a single extrusion stage as in Fig. 1 with a large opening angle, only a partial volume is formed per extrusion increment. This should lead to a constant extrusion progress when impulses with constant energy are applied and the sample is in full contact with the die. However, by changes in forming channel, changes in energy transmission are expected, that need to be understood for use of the process.

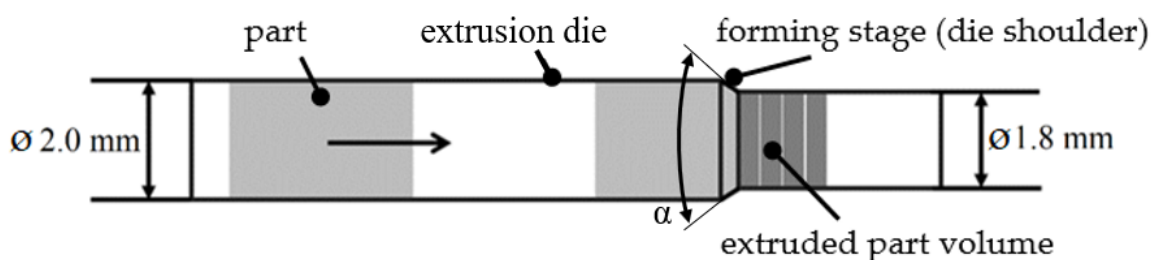


Figure 1: Full-forward extrusion with large opening angle α

In this paper, the influence of increased forming channel length and changed channel paths geometry on the energy transmission was investigated. The die shoulder was enlarged and the opening angle α was reduced. Hence, the whole part volume was increasingly strained, which led to a change in the curve of energy as a function of the extrusion depth. The extrusion process was analytically modelled and compared to experimental results.

2 Materials and Methods

2.1 Set-up

In this paper, full-forward extrusion of EN AW-6061 aluminum alloy prismatic parts was investigated in forming channels with aspect ratios higher than 10. Starting with a straight reference channel, where the part is full-forward extruded according to the height profile (Fig. 2), additional changes of the forming channel path geometry were applied. By comparing the forming progress, the influence of channel depth and path geometry on energy transmission was investigated.

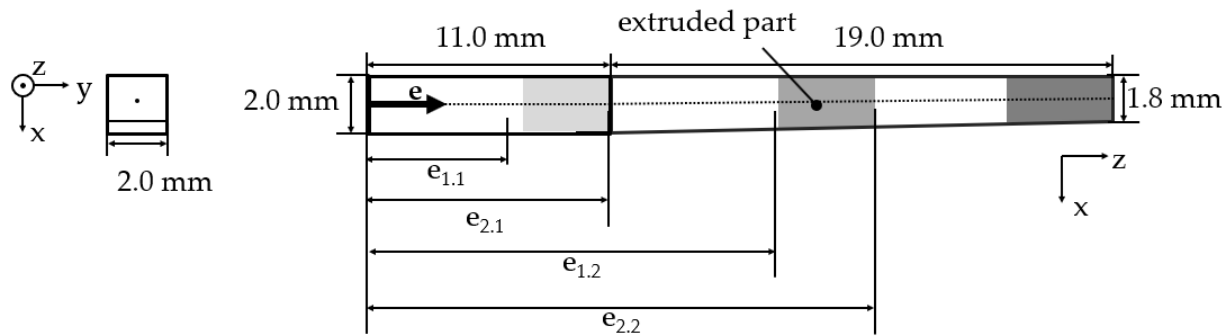


Figure 2: Height profile of forming channels (full-forward extrusion)

This height profile starts with constant height of 2 mm over a length of 11 mm. From this point to the total length of 30 mm, the height is reduced from 2.0 mm to 1.8 mm while the width of the channel is kept constant at a value of 2.0 mm. All formed parts – dimensioned $2 \times 2 \text{ mm}^2$ in cross-section and 4 mm in samples initial length L_0 – were placed at the same starting point of $e_{1,1} = 7 \text{ mm}$ (left side of sample) and $e_{2,1} = 11 \text{ mm}$ (right side of sample).

Shock waves were caused in distilled water iteratively by vaporizing aluminum wires with a diameter $d_w = 0.5 \text{ mm}$ and a length of $l_w = 20 \text{ mm}$. A loading voltage $U_0 = 3 \text{ kV}$ and a capacity $C = 100 \mu\text{F}$ supplied a loading energy $E_C = 450 \text{ J}$. The parts were formed incrementally through the forming channels. The general setup is illustrated in Fig. 3a. The forming die was assembled by replaceable forming elements. Multi-stage forming dies were additionally equipped with a window-plate for direct optical access, Fig. 3b.

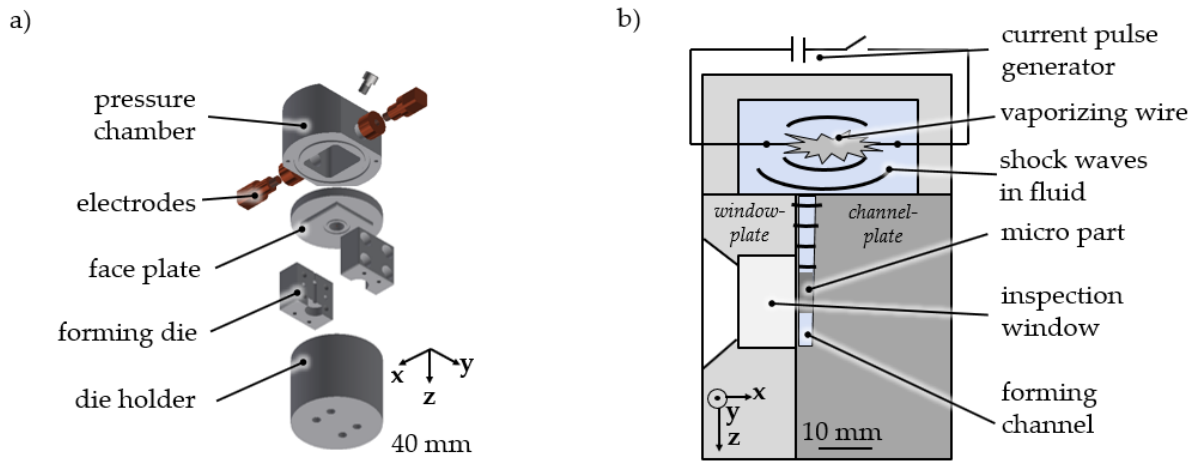


Figure 3: Forming set-up; a) general assembly (die according to Fig. 1), b) multi-stage channel (dies according to Fig. 4)

A 10 mm thick sapphire pane as part of the window-plate gave optical access to the forming zone to measure the position and length of the parts between forming increments. Hence, forming was performed directly at the sapphire pane. Four different channel path geometries were realized, Fig. 4.

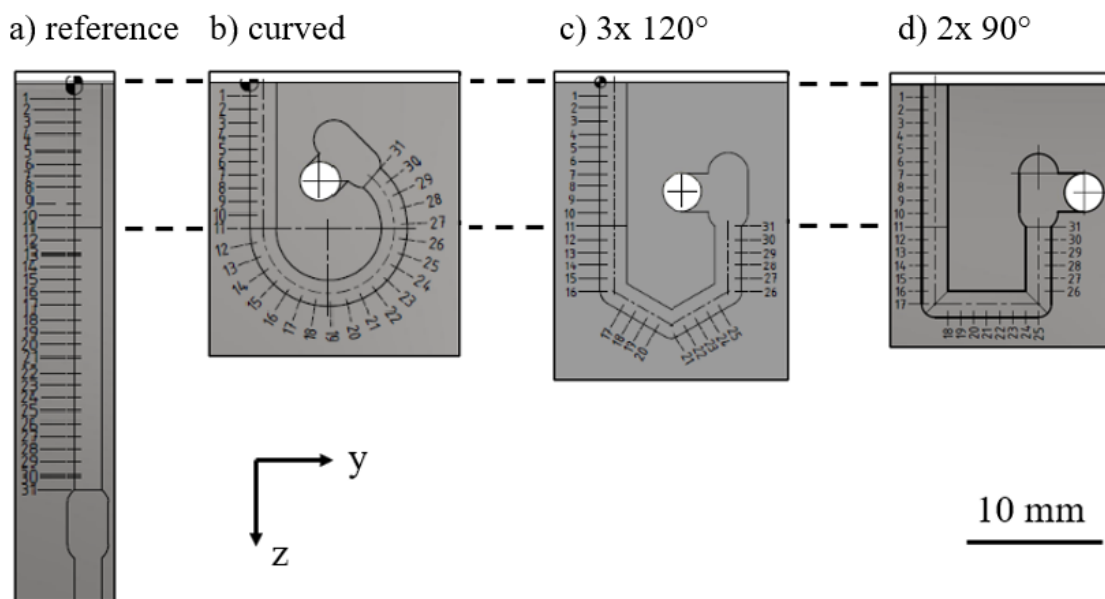


Figure 4: Channel path geometries; a) straight reference channel, b) curved channel, c) 3x120° angular channel, d) 2x90° angular channel

In all forming channels, the micro parts were extruded with the same height profile (cf. Fig. 2). In addition to the reference channel, within the three other channels the micro parts undergone a further simultaneously forming by curvature of the channel or by angular redirection (120° and 90°). The position of the part was measured through the optical access in situ with a digital microscope (Leica DVM6). Due to diffraction at the edge of the lid, the

recording area of the microscope had to be moved to follow the part. The supplied energy was calculated by the measured loading voltage and the nominal capacity of the current pulse generator.

2.2 Analytical modelling

For analytical modelling, full forward extrusion according to (Doege et al., 2010) was considered, equation 1.1. The material strain behavior was represented by a flow curve (yield stress k_f depending on the true plastic strain φ) according to (Lange et al., 2008). The strain was calculated based on the channel geometry that cause a lengthening dL of the part along the extrusion depth e . The performed work W (W_{id} – ideal forming work; W_{rs} – friction work at channel shoulder surface; W_{rw} – friction work at channel surface; W_{loss1} – work losses) along the extrusion depth e with changing cross-sectional area A of the forming channel was calculated by equation 1.2., whereby the losses in electrohydraulic extrusion caused by friction as well as for example by the shock wave generation and propagation were summarized in the term W_{loss2} .

$$W_{ges} = W_{id} + W_{rs} + W_{rw} + W_{loss1} = W_{id} + W_{loss2} \quad (1.1)$$

$$W_{ges} = \int_0^{e_{end}} (A k_f \varphi) de + W_{loss2} \quad (1.2)$$

$$W_{ges} = \int_0^{e_{end}} \left((2 \tan(\alpha) e) \cdot k_f \cdot (\ln(1 + dL/L_0)) \right) de + W_{loss2} \quad (1.3)$$

With the assumption that the reflections of the driving shock wave are too low to contribute to the forming progress, only a portion of the loading energy is acting according to the ratio of affected part surface (4 mm²) and inner chamber surface ($\approx 10,000$ mm²). Hence, in the following the supplied energy ΣE_i is roughly determined via $\Sigma E_i = i \cdot E_C/2500$.

3 Results

For extrusion through forming channels, the sapphire pane withstood the dynamic loads and enabled continuous observation of the forming progress, Fig. 5a. The shock wave followed the curvature of the geometry of channels up to 180°, Fig. 5b. However, as the camera had to follow the part while forming, the relative position within the taken pictures changed with the extrusion depth.

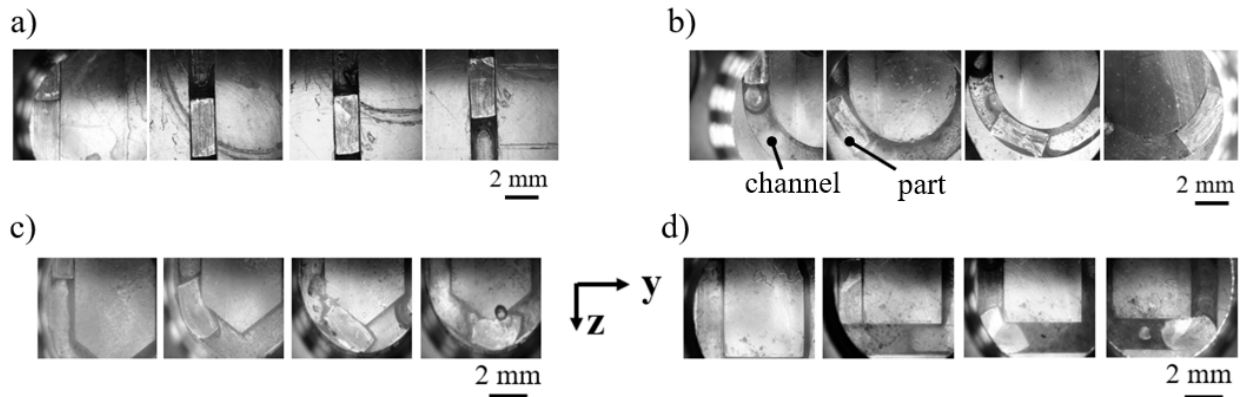


Figure 5: Forming proceed: a) reference channel, b) curved channel, c) 3x120° angular channel, d) 2x90° angular channel

The energy-displacement curve of the reference channel was calculated with equation 1.2. The ideal work for full-forward extrusion results in a non-linear energy-displacement curve, cf. Fig. 6a. The experimental results are in good agreement to the analytical results, cf. Fig. 6b. Hence, work losses by channel depth are assumed to be low.

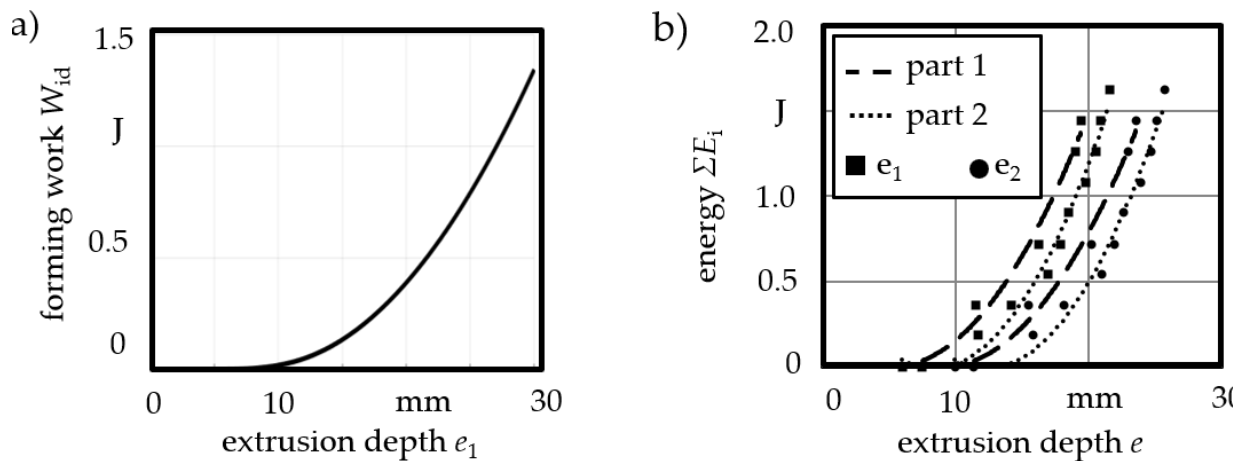


Figure 6: Straight reference channel; a) calculated ideal forming work, b) experimental results

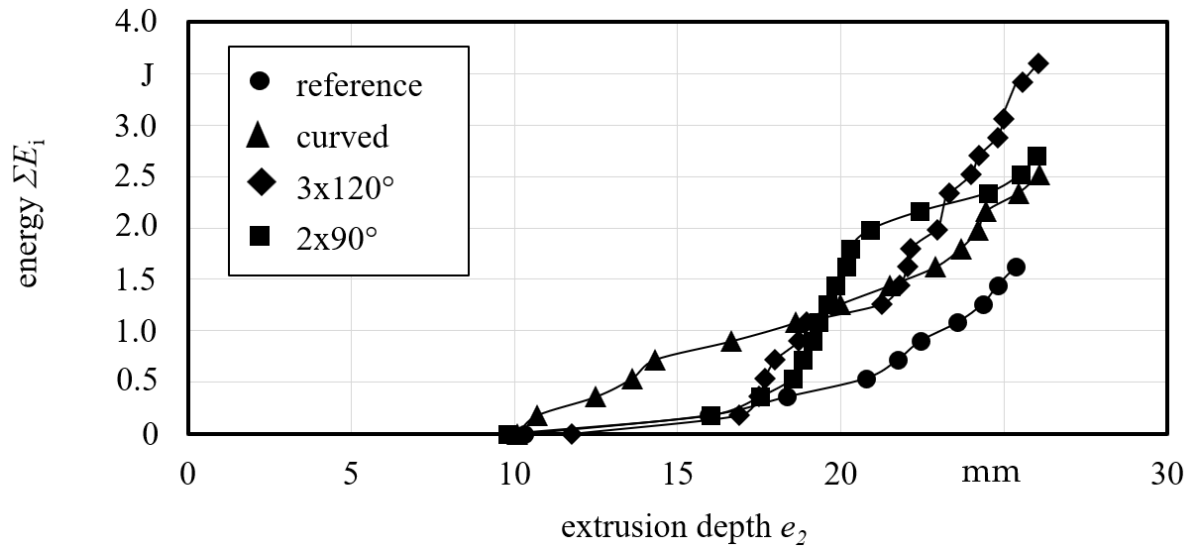


Figure 7: Energy-displacement curves

Comparing the straight reference channel with the other channels, a change in the energy-displacement curve can be observed, Fig. 7. Due to additional forming of the micro part, higher forming energies were required for the progress of the part in the channel which correlates with a decrease of step size $\Delta e = e_{2,i} - e_{2,i-1}$ within the curved zone ($11 \text{ mm} < e_2 < 15 \text{ mm}$), Fig. 8a.

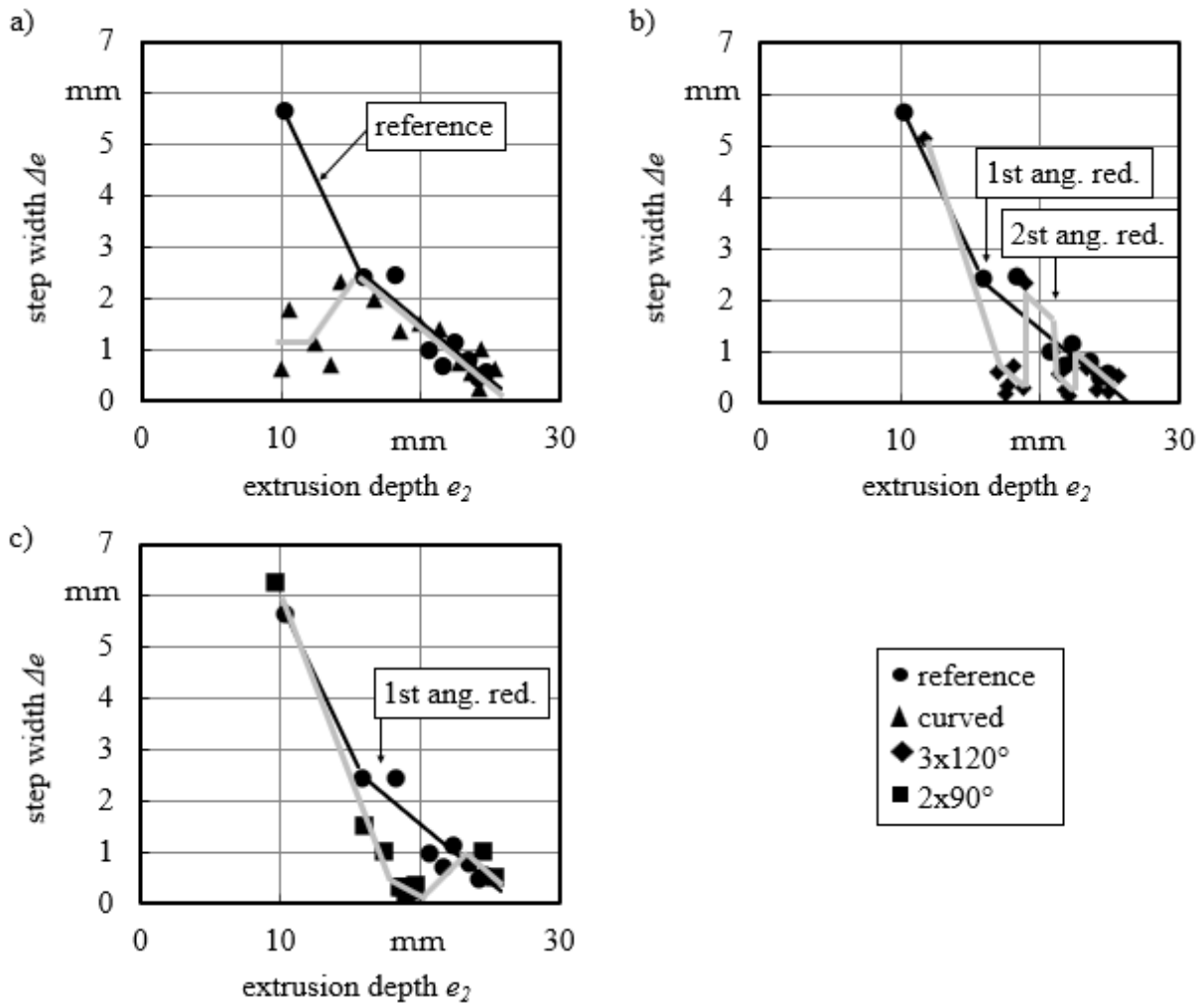


Figure 8: Step width Δe ; a) reference – curved, b) reference – 3x120°, c) reference – 2x90°

At the same time, it should be emphasized that as soon as the bending in the curved channel is completed, the graph follows the same path like the straight reference channel. Hence, the forming progress is dominated by the forming energy needed and not by the redirection of the shock wave. The same behavior holds for the angular channels at first and second angular redirections (1st and 2nd ang. red.), cf. Fig. 8b and 8c. The both deliver the same sample progress as the reference channel while the forming is determined by the height profile. The energy transmission in the depth of the channels did not change despite further undercuts.

An exemplary photo series with 30 frames per second is shown for the 2x90° angular channel, Fig. 9. Here, light emission by wire explosion as well as an occurrence of gas bubbles in the pressure transmitting fluid was detected. The bubbles were passing the micro part after extrusion (flow). Thus, the energy was transmitted well even without a complete sealing between channel and part and even with the transient appearance of compressible gas bubbles.

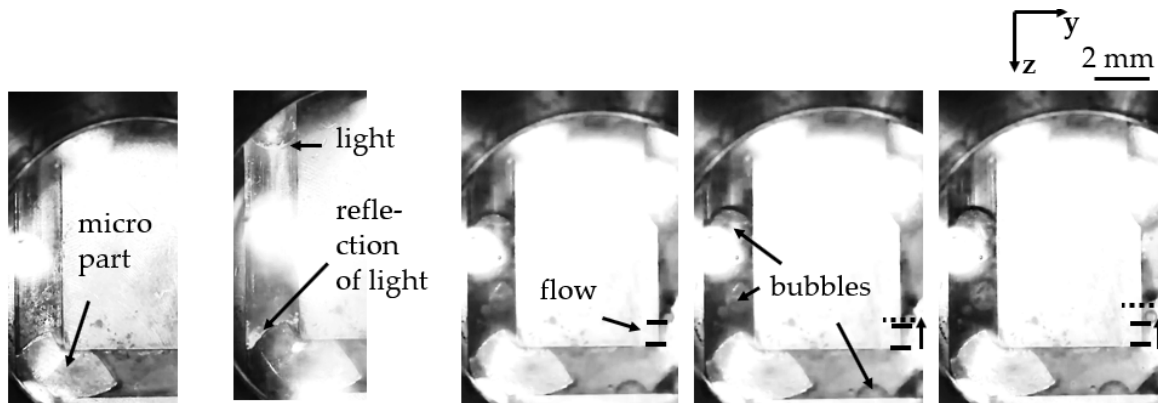


Figure 9: In-process measurement – detection of light emission, flow, bubbles

4 Conclusion

EN AW-6061 aluminum alloy parts were incrementally extruded in forming channels with high aspect ratio and different geometric channel paths by electrohydraulic impulses. The optical access as part of the extrusion die enabled process observations. Four different channel path geometries with continuous extrusion and additional forming steps were investigated and the energy transmission in the depth of the channel was examined. Following conclusions are drawn:

- depth of forming channels was identified to have low influence on energy transmission
- curvature and angle of forming channels path was identified to have low influence on energy transmission
- energy transmission by shock wave was possible even without a complete sealing between channel and formed part
- energy transmission by shock wave was constant even with fluctuations of incompressibility by gas bubbles

These findings confirm the potential of high aspect ratio forming channels as a promising technology for micro production without handling operations between multiple forming stages.

Acknowledgements

The authors would like to gratefully acknowledge the financial support of the Collaborative Research Center SFB 1232 "Farbige Zustände" by the German Research Foundation (DFG).

References

Doege, E.; Behrens, B.-A.: Handbuch Umformtechnik – Grundlagen, Technologien, Maschinen. Springer Verlag (2010).

- Fan, W. F.; Li, F.: Study on Blanking Force of Fine-Blanking with Negative Clearance and Common Blanking for AISI-1045 through Simulation and Experiment Methods. *Materials Science Forum* 704–705, (2011) 1175–1179, DOI: 10.4028/www.scientific.net/MSF.704-705.1175
- Lange, L.: *Umformtechnik Handbuch für Industrie und Wissenschaft – Band 4: Sonderverfahren, Prozesssimulation, Werkzeugtechnik, Produktion*. Springer-Verlag, Berlin, Heidelberg, 1993.
- Lange, K.; Kammerer, M.; Pöhlandt, K.; Schöck, J.: *Fließpressen. Wirtschaftliche Fertigung metallischer Präzisionswerkstücke*. Springer-Verlag, Berlin, Heidelberg, 2008.
- Langstädtler, L.; Schönemann, L., Schenck, C.; Kuhfuss, B.: Electromagnetic Embossing of Optical Microstructures, *J. Micro Nano-Manuf.* (2016)
- Langstädtler, L.; Pegel, H.; Beckschwarte, B.; Herrmann, M.; Schenck, C.; Kuhfuss, B.: Electrohydraulic incremental bulk metal forming, *MATEC Web of Conferences* 190 (2018) 3001 DOI: 10.1051/mateconf/201819003001
- Langstädtler, L.; Pegel, H.; Beckschwarte, B.; Herrmann, M.; Schenck, C.; Kuhfuss, B.: Flexible tooling for impulse forming, *Procedia Manufacturing* 27 (2019) 130-137 DOI: 10.1016/j.promfg.2018.12.055
- Langstädtler, L.; Schnabel, S.; Herrmann, M.; Schenck, C.; Kuhfuss, B.: Short-Term Material Characterization by Electrohydraulic Incremental Extrusion through Micro Channels, *Materials 14 - 3* (2021), DOI: 10.3390/ma14030525
- Liu, Y. X.; Hua, L.; Lan, J. A.; Wei, X.: Studies of the deformation styles of the rubber-pad forming process used for manufacturing metallic bipolar plates. *J Power Sources* 195(24) (2010) 8177–8184, DOI: 10.1016/j.jpowsour.2010.06.078
- Stöbener, D.; Alexe, G.; Langstädtler, L.; Herrmann, M.; Schenck, C.; Fischer, A.: An optical method to determine the strain field on micro samples during electrohydraulic forming, *Procedia CIRP* 87 (2020), 438-443, DOI: 10.1016/j.procir.2020.02.099
- Vollertsen, F.; Friedrich, S.; Kuhfuß, B.; Maaß, P.; Thomy, C.; Zoch, H.-W: *Cold Micro Metal Forming. Chapter 4.1 – Introduction to Tooling*, Bremen, Germany, Springer Verlag, 2020
- Mahshid, R.; Hansen, H. N.; Arentoft, M. Characterization of precision of handling system in high performance transfer press for micro forming. *Manufacturing Technology*, 63 (2014), 497-500, DOI: 10.1016/j.cirp.2014.03.001